

Influence of Intraluminal Thrombus Topology on AAA Passive Mechanics

F Riveros¹, G Martufi², TC Gasser³, JF Rodriguez^{1,4}

¹Aragon Institute of Engineering Research, University of Zaragoza, Spain

²The University of Calgary, Canada

³Royal Institute of Technology (KTH), Sweden

⁴CIBER de Bioingeniería, Biomateriales y Nanomedicina (CIBER-BBN), Zaragoza, Spain

Abstract

An intraluminal thrombus (ILT) is found in most AAAs of clinically relevant size. Even though some studies seem to indicate a protective role of the ILT against AAA rupture, there is still great controversy on this regard. In addition, patient-specific AAA models are generated from gated medical images in which the artery is under pressure. Identification of the AAA zero pressure geometry would allow for a more realistic estimate of the aneurysmal wall mechanics and a better understanding of the role of the ILT. This study looks into the influence of the ILT on patient specific AAA accounting for the zero pressure geometry. Ten patient specific AAA of similar maximum diameter (4.8-5.2cm) and ILT volume were considered. For the stress analysis, the arterial wall is modeled as an anisotropic hyperelastic solid. Our results suggest that the geometrical configuration of the ILT relative to the arterial wall may be an influential factor not only on the ensuing peak wall stress, but also on its location within the lesion. The effects of the ILT topology are enhanced when the zero pressure configuration of the lesion is accounted for, where as the location of the peak wall stress in the lesion corresponds to the region of minimal ILT thickness. These suggest that the topology of the ILT, which greatly influence the zero-pressure geometry of the AAA, affects the stress field at the systolic pressure on AAA.

1. Introduction

An abdominal aortic aneurysm (AAA) is an abnormal widening of the aorta, commonly developed below the renal arteries and above the iliac bifurcations. The progressive aortic enlargement that takes place during aneurysmal disease combined with weakening of the wall tissue may result in aortic rupture [1]. Although the criterion for AAA repair varies in practice, the maximum diameter is the most frequently used clinical AAA repair indication. However, the diameter criterion is under contro-

versial discussion since only 25% of AAAs rupture in a patients lifetime [2]. Therefore, alternative rupture risk indices based on biomechanical parameters like peak wall stress (PWS) or peak wall rupture risk (PWRR) have been proposed in order to target patients that require AAA repair [3–5]. The computation of such parameters requests a reliable reconstruction of the aortic geometry, appropriate material properties for the aneurysmatic tissues, and a properly understanding of the role of each structural element that composes the aneurysm. The experimental study by vande Geest et al. [6] demonstrated that the aneurysmal degeneration of aortic tissue leads to an increase in mechanical anisotropy, with the circumferential direction being stiffer. The reconstructed AAA geometry from CT images, for most CT modalities, refers to the configuration that is inflated with the diastolic blood pressure. Considering this geometry as the zero-pressure configuration, leads to incorrect deformations and stresses relative to the in-vivo condition as was demonstrated in [7]. Therefore, a more realistic computation of the PWS should consider such a zero-pressure configuration. A recent work by our group has proposed an efficient algorithm to find the zero pressure configuration of AAA [7] such that when loaded with the diastolic pressure, the deformed AAA matches the AAA geometry seen in the CT images. This study looks into the influence of the ILT on the stress field on patient specific AAA accounting for the zero pressure geometry in order to gain a better understanding on the structural role of the ILT in the load bearing capacity of a AAA.

2. Methods

2.1. Image acquisition and 3D reconstruction

Ten non-ruptured AAA geometries, were acquired at two hospitals in Stockholm, Sweden. All AAA images provided a sufficiently high out-of-plane resolution of the image data and a good identification of the exterior aneurysm surface. Local ethics committee approved

the collection and use of anonymized data from human. Aneurysms geometries were reconstructed with the diagnostic software A4clinics Research Edition (VASCOPS GmbH, Graz, Austria), which was applied by an operator with engineering background assisted by a radiologist to ensure proper segmentation of the aneurysms. Details regarding the image segmentation process are given elsewhere [8]. All reconstructed models include the ILT and assumed a non-homogeneous aneurysm wall thickness varying between 1.5 mm and 1.13 mm at the thrombus-free and covered sites respectively [9].

2.2. Material model

We consider the material of the aneurysm wall and ILT as hyperelastic. The aneurysmal wall tissue was modeled by means of the transversally isotropic SEF [10]:

$$W_{\text{wall}}^{\text{aniso}} = \kappa(J-1)^2 + D_1 \left(e^{(D_2(\bar{I}_1-3))} - 1 \right) + \frac{k_1}{k_2} \left(e^{(k_2(\bar{I}_4-1)^2)} - 1 \right), \quad (1)$$

where D_1 , D_2 , k_1 , k_2 are material parameters and κ is the volumetric modulus; $J = \det \mathbf{F}$ is the volume ratio with \mathbf{F} the deformation gradient; $\bar{I}_1 = \text{tr} \bar{\mathbf{C}}$, $\bar{I}_4 = \mathbf{a}_0 \cdot \bar{\mathbf{C}} \cdot \mathbf{a}_0$ are the first and fourth invariants of the modified right Cauchy-Green tensor, $\bar{\mathbf{C}} = \bar{\mathbf{F}}^T \bar{\mathbf{F}}$, with $\bar{\mathbf{F}} = J^{-1/3} \mathbf{F}$ and \mathbf{a}_0 a unit vector along the direction of anisotropy. This approach was used due to the lack of histologic evidence regarding the fiber distribution in aneurysmal tissue. The wall's stiffer response corresponds to its circumferential direction, as it has been verified through biaxial testing in Vande Geest et al. [6]. The material parameters were obtained by means of a nonlinear regression analysis of the mean biaxial test for aneurysmal tissue reported in van de Geest et al [6]. Table 1 shows the identified model.

Table 1. *Model parameters for the constitutive model given in Eq. 1.*

D_1	D_2	κ	k_1	k_2	R^2
kPa	-	kPa	kPa	-	-
0.214	41.3	10^4	0.212	130	0.95

The ILT has been modeled as an isotropic hyperelastic material with the SEF proposed by Di Martino and Vorp [11]:

$$W_T = C_{20}(\bar{I}_2 - 3) + C_{02}(\bar{I}_2 - 3)^2, \quad (2)$$

where C_{20} and C_{02} are material constants with dimensions of stress and $\bar{I}_2 = 0.5((\text{tr} \bar{\mathbf{C}})^2 - \text{tr} \bar{\mathbf{C}}^2)$ the second modified invariant of $\bar{\mathbf{C}}$. The reported parameters used were $C_{20} = 28$ kPa and $C_{02} = 28.6$ kPa.

2.3. Finite element model

Each geometry was discretized with linear tetrahedrons and nearly isotropic meshes. The total number of elements per AAA model ranged between 400000 and 600000 elements, and had at least three elements across the arterial wall thickness in order to capture the stress gradients in the wall. To test the quality of the mesh used for the calculations, a sensitivity analysis was performed on one model subject to diastolic pressure. This study demonstrated (results not shown) that for meshes of more than 300,000 elements, the maximum principal stress changes less than a 3% with respect to the finest mesh used, while giving a sufficient number of elements through the arterial wall.

The anisotropic material model for the arterial wall was implemented in the material user subroutines UANISO-HYPER_INV within the finite element software SIMULIA abaqus (Dassault Systems). The constraints due to the thoracic aorta and common iliac arteries were simulated by restraining the longitudinal displacement while allowing displacements in the radial direction.

The assessment of the direction of anisotropy has been performed following the procedure proposed by Alastrue et al.[12]. In this procedure, the model is subjected to a sub-diastolic pressure using the isotropic part of the material model described by Eq. (1). Then, the direction of anisotropy is made coincident with the direction of maximum principal stress. The result obtained with this procedure is a dominant circumferential direction of the fibers (see [7] for details).

Internal pressures of 10.6 kPa (80 mmHg) and 16 kPa (120 mmHg) were applied to the lumen surface to simulate the diastolic and systolic pressures, respectively. The diastolic pressure was used during the iterative algorithm to find the zero-pressure configuration, as this was considered the intraluminal pressure when the images were acquired. The systolic pressure was used to find the largest stresses on the AAA.

2.4. Zero pressure geometry algorithm

The algorithm to reconstruct the zero-pressure geometry of an AAA model from the CT image based geometry is detailed in [7]. The main purpose of this algorithm is to find a reference configuration that deforms into the geometry $\mathbf{X}_{\text{image}}$ that is seen in the CT images when subjected to the diastolic pressure, P_{diast} . The proposed algorithm keeps the mesh connectivity unchanged and iteratively updates the nodal coordinates. When working with the anisotropic material, the local circumferential direction is also consistently pulled-back to the zero-pressure configuration.

3. Results

3.1. Zero pressure geometry

The influence of the ILT on the zero pressure configuration is shown in Figure 1 where the CT based and zero pressure models are depicted. In the areas where the ILT is not present, or has a minimum thickness, the arterial wall shows a larger contraction with respect to the CT based image due to the larger compliance of the aneurysmal wall.

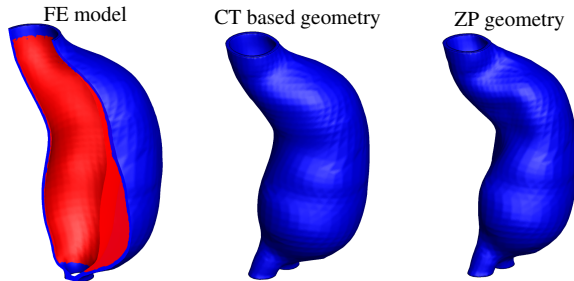


Figure 1. CT-based, Zero-pressure based geometries and initial FE model of one of the patients.

3.2. Stress field

In all ten geometries, the PWS using the CT-based geometries was underestimated by a 14% (SD 14%) with respect to PWS obtained with the zero pressure geometry as demonstrated in [7] and shown in Figure 2. In addition, a two-sided signed rank statistical test shows that computations based on the zero-pressure geometry will predict a larger PWS than based on the CT-based geometry with larger probability ($p = 0.005$).

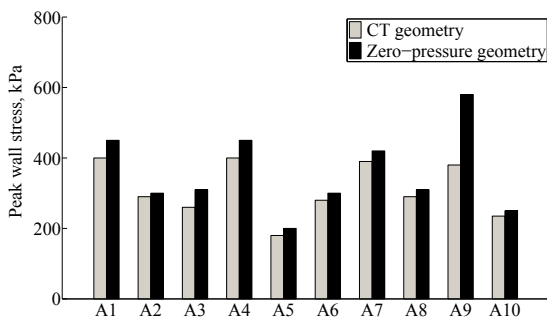


Figure 2. Predicted PW stress for the CT-based (gray bars) and ZP based (black bars) reference configurations.

The influence of the ILT in the PWS field is clearly shown in Figure 3. The areas of the AAA that are not covered by the ILT, or where the ILT is thinner, show a considerable higher value of the peak wall stress. This feature is enhanced when the zero pressure configuration is accounted for in the analysis.

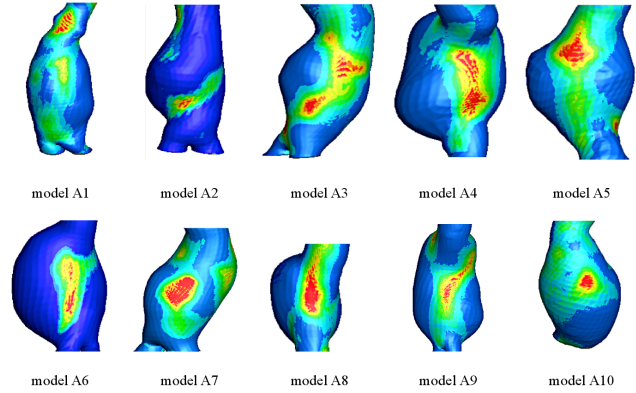


Figure 3. PW stress for the ZP-based reference configuration for all AAA models.

A more detail observation of the PWS field in each AAA model is depicted in Figure 4.

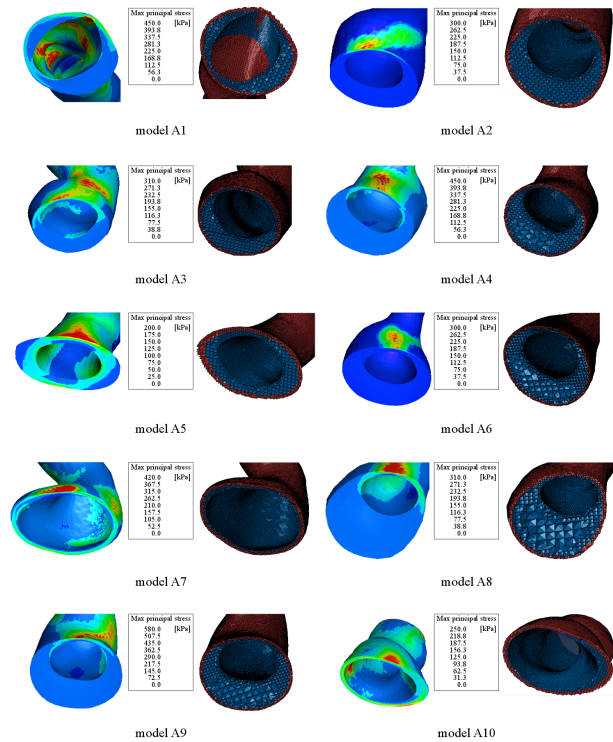


Figure 4. Location of PW stress for the ZP-based reference configuration for all AAA models.

This figure demonstrates that PWS is always located at the point where the ILT thickness is minimum, or at the bared wall when the ILT does not completely cover the inner arterial wall. Further, the results shown that when the ILT thickness distribution around the arterial wall is heterogeneous (minimum to maximum ILT thickness ratio less than 10%) the PWS was located in the region of minimum ILT thickness independent of AAA wall curvature (8

of 10 cases). However, in those cases where the ILT thickness was more uniformly distributed (minimum to maximum ILT thickness ratio larger than 30%), the PWS was located on sites where the ILT was thinner but on areas of relatively high curvature (models A5 and A7).

4. Discussion and conclusion

The present work makes use of a novel methodology to predict the zero-pressure geometry of patient-specific AAAs for improving the estimation of PWS on patient specific geometries of AAA. This primary step overcomes one of the main limitations of current AAA stress analysis, i.e. that models that use the CT-based geometries underestimate PWS [13–15].

Our previous research has shown that the material behavior of the wall, i.e. isotropic versus anisotropic, has little influence on the PWS [7]. However, remarkable changes are observed when the reference configuration is changed from the CT-based to the ZP-based (see Figure 2). This study also demonstrates that the presence and morphology of the ILT influence the PWS field of the AAA, since the ILT modifies the compliance of the AAA (arterial wall and ILT). More specifically, our results show that when the ILT thickness distribution is non uniform along the arterial wall, with minimum to maximum ILT thickness lower than 10%, the PWS is located in the region of minimal ILT thickness regardless of the AAA wall curvature. An effect that is enhanced when the ZP geometry is taken as the reference configuration. However, if the ILT thickness distribution is more uniform, even though the PWS still appears in an area of minimum ILT thickness, it appears to be better correlated with the AAA wall curvature. This is probably due to the fact that a more uniform ILT thickness distribution along the arterial wall, leads to a more uniform compliance distribution of the AAA wall, in addition to a more homogeneous distribution of the pressure to the wall. This will be equivalent to a case of an AAA without the presence of ILT where the geometric features of the AAA govern the location of the PWS. We are conducting simulations on an additional set of ten patients in order to further demonstrate these observations. However, these results indicate that in addition to AAA morphology and local wall curvature, ILT morphology is of key importance for the AAA rupture risk assessment.

References

- [1] N. S, Limet R, Defawe O. Abdominal aortic aneurysm. *Lancet* 2005;365:1577–1589.
- [2] Brown L, Powell J. Risk factors for aneurysm rupture in patients kept under ultrasound surveillance. uk small aneurysm trial participants. *Ann Surg* 1999;230(3):289–296.
- [3] Truijers M, Pol J, Schultzekool L, van Sterkenburg S, Fillinger M, Blankensteijn J. Wall stress analysis in small asymptomatic, symptomatic and ruptured abdominal aortic aneurysms. *Eur J Vasc Endovasc Surg* 2007;33(4):401–407.
- [4] Gasser T, Auer M, Labruto F, Swedenborg J, Roy J. Biomechanical rupture risk assessment of abdominal aortic aneurysms: Model complexity versus predictability of finite element simulations. *Eur J Vasc Endovasc* 2010;40:176–185.
- [5] Maier A, Gee M, Reeps C, Pongratz J, Eckstein H, Wall W. A comparison of diameter, wall stress, and rupture potential index for abdominal aortic aneurysm rupture risk prediction. *Ann Biomed Eng* 2010;38:3124–3134.
- [6] Vande Geest J, Sacks M, Vorp D. The effects of aneurysm on the biaxial mechanical behavior of human abdominal aorta. *J Biomech* 2006;39:2347–2354.
- [7] Riveros F, Chandra S, Finol E, Gasser T, Rodriguez J. A pull-back algorithm to determine the unloaded vascular geometry in anisotropic hyperelastic aaa passive mechanics. *Ann Biomed Eng* 2013;41(4):694–708.
- [8] Auer M, Gasser T. Reconstruction and finite element mesh generation of abdominal aortic aneurysms from computerized tomography angiography data with minimal user interactions. *IEEE Trans Med Imaging* 2010;29(4):1022e8.
- [9] Larsson E, Labruto F, Gasser T, Swedenborg J, Hultgren R. Analysis of aortic wall stress and rupture risk in patients with abdominal aortic aneurysm with a gender perspective. *J Vasc Surg* 2011;54(2):295–299.
- [10] Rodriguez J, Ruiz C, Doblaré M, Holzapfel G. Mechanical stresses in abdominal aortic aneurysms: influence of diameter, asymmetry, and material anisotropy. *ASME J Biomech* 2008;130(2):021023.
- [11] Di Martino E, Vorp D. Effect of variation in intraluminal thrombus constitutive properties on abdominal aortic aneurysm wall stress. *Ann Biomed Eng* 2003;31(7):804–809.
- [12] Alastrué V, García A, Peña E, Rodríguez J, Martínez M, Doblaré M. Numerical framework for patient-specific computational modelling of vascular tissue. *Commun Numer Meth En* 2010;6:1–30.
- [13] De Putter S, Wolters B, Ruttena M, Breeuwer M, Gerritsen F, van de Vosse F. Patient-specific initial wall stress in abdominal aortic aneurysms with a backward incremental method. *J Biomech* 2006;40:1081–1090.
- [14] Lu J, Zhou X, Raghavan M. Inverse elastostatic stress analysis in pre-deformed biological structures: demonstration using abdominal aortic aneurysms. *J Biomech* 2007;40:693–696.
- [15] Speelman F, Bosboom G, Schurink J, Buth M, Breeuwer M, Jacobs M, et al. Initial stress and nonlinear material behavior in patient-specific aaa wall stress analysis. *J Biomech* 2009;42(11):1713–1719.

Address for correspondence:

Jose F. Rodriguez
 Mechanical Engineering department / University of Zaragoza
 Edf. Betancourt, Maria de Luna S/N / 50018 Zaragoza / Spain
 jfrodri@unizar.es